Hindawi
Mobile Information Systems
Volume 2022, Article ID 1456425, 12 pages
https://doi.org/10.1155/2022/1456425

Research Article

Fault Identification and Analysis of Communication Network Based on Deep Learning

Caiying Feng and Yan Zhao

College of Information and Electronic Engineering, Shangqiu Institute of Technology, Shangqiu 476000, Henan, China

Correspondence should be addressed to Caiying Feng; 1350007066@sqgxy.edu.cn

Received 9 May 2022; Revised 8 June 2022; Accepted 15 June 2022; Published 23 August 2022

Academic Editor: Le Sun

With the wide application of communication, the role of communication network is becoming more and more important. The current network maintenance methods are still limited to regular maintenance and post-maintenance, do not have a complete network status monitoring function, cannot evaluate the network status, and it is difficult to maintain before the serious deterioration of the network. Network faults can only be solved by the professional knowledge of technicians, and the maintenance efficiency is not high, so it is impossible to diagnose and locate errors in time and accurately, and eventually it will be repaired forcibly at the cost of replacing network cables. This paper introduces the network fault analysis, then, deep learning is used to model the fault diagnosis of communication network, finally, in the experimental part, the results of fault location are analyzed, and several methods are compared. The simulation results show that the proposed method avoids the errors caused by the generated model to a certain extent, and improves the robustness, universality and accuracy of the network fault diagnosis model.

1. Introduction

In this paper, we propose to learn a series of high-level function representations through deep learning, that is, the so-called deep hidden identity function, for face verification. Any most advanced classifier can learn based on these high-level representations for face verification [1]. This paper shows how these traditional methods cannot explain why large neural networks have become so common in practice, but our experiments show that advanced image classification convolution networks trained by random gradient methods are easily compatible with random symbols. Compared with the traditional model, our experimental findings can be explained [2]. Deep learning algorithms, especially convolution networks, have rapidly become a popular method for analyzing medical images. This paper discusses the key concepts in deep learning related to medical image analysis, and summarizes some contributions to this field, most of which appeared in the past year, and discusses the open challenges and trends of future research [3]. Here, we show that sequence specificity can be determined from experimental data by deep learning technology, which provides an extensible, flexible and unified calculation method for pattern discovery. Using various experimental data and evaluation indicators, we find that deep learning is superior to other most advanced methods [4]. We propose a new deep convolution neural network structure, which is inspired by foresight, and the foresight module is replaced by deep divisible convolution [5]. Point cloud is an important geometric data structure. In this paper, we design a new neural network, which uses point cloud directly and respects the arrangement variance of access points well. [6]. This paper shows how the nonlinear semi-supervised embedding algorithm is used together with the "shallow" learning technology. This technique provides a simple semi-supervised deep learning, while generating competitive error rates compared with these methods and the existing shallow semi-supervised technology [7]. Accurate and timely traffic flow information is very important for the successful deployment of intelligent transportation system. This paper proposes a new traffic flow prediction method based on deep learning, which inherently considers temporal and spatial correlation. By observing the research results, we can know that the traffic flow forecasting method proposed in this paper has better forecasting performance; [8]. In recent years, network has developed rapidly in

industrial and medical fields. NB-IoT is a wireless communication and low-power broadband technology based on new Internet of Things devices, which enables various services to grow. Its performance analysis and simulation results show that this detection mechanism can improve transmission efficiency and effectively reduce network communication failure power consumption [9]. With the rapid expansion of satellite communication, more and more unattended ground terminals are expanding outward to serve local customers. In this paper, the signal-to-noise ratio (SNR) signal behavior measured by grounding terminal is associated with different types of possible faults, and a terminal fault identification (TFI) system is proposed. Through the analysis of actual data, the effectiveness of this method is verified [10]. Microcomputer protection marks the intelligent era of protection devices. This paper studies the abnormal interruption analysis of protection channels based on the data of relay protection and recording management system (PFRMS) and communication network management system (CNMS) [11]. With the rapid increase of the scale and complexity of communication networks, this paper proposes an efficient alarm association and fault identification scheme based on OSI management object classes to quickly separate fault sources. The algorithm uses managed object class dependency graph, observing the research results, we can see that the proposed algorithm is simple to implement [12]. The principle and algorithm of Wide Area Protection System (WAPS) have been developed greatly. This paper presents a reliability evaluation method for large-scale secure communication systems. Finally, CSWAP in IEEE 11-bus system is analyzed as an example, and the factors affecting the reliability of CSWAP are summarized, which verifies the effectiveness of this method [13]. The complexity of communication networks and the amount of information transmitted in these networks make it more and more difficult to manage these networks. In this paper, a new event association scheme for fault identification of communication networks is proposed, which is based on algebraic operation of sets [14]. In this paper, a new method of fault data identification based on subbasis function is proposed, and a pre-whitening matching detection method of underwater ship communication network is proposed. The underwater ship communication network model and communication channel model are established, and the fault data signal is decomposed into multiple narrowband signals, which can effectively improve the underwater communication quality [15].

2. Network Fault Analysis

From the perspective of network slicing, the network architecture is shown in Figure 1. Based on the system model, we summarized the common network errors, as shown in Table 1.

It can be seen from Table 1 that NFV concept and network slicing are more prominent features of 5G than 4G, so the deployment of 5G network should also consider the possible interruptions in these areas and take precautions in advance. With the introduction of network slicing technology, the following issues need attention:

2.1. Granularity. Slicing can meet the needs of different online services and different user groups. However, the number of slices and the cutting method are the problems that need to be solved when slicing. In addition to being large enough to provide sufficient flexibility, slicing units may not meet the requirements of certain types of networks, while slicing units are too small to manage and deploy.

2.2. Flexibility. If slicing can be used very flexibly, it has some real-time performance, just like 4G policy control architecture. However, slicing is too flexible, and the cost and risk of network management increase slightly. After all, stability and reliability are also issues that need to be considered in network management. In addition, the launch of new services is not achieved overnight, which requires a lot of business preparation and analysis.

2.3. Allocation of Resources. The application of network slicing technology complicates the operation of network. Operators must be able to quickly configure network resources in the shortest time according to customer needs and provide highly compatible services flexibly. Failure to configure network resources in time will lead to network congestion.

2.4. Isolation. Network slicing technology must support the isolation of various network components. If the slab does not meet the insulation requirements, the performance of other parts will be affected.

Observing Table 1 shows that the fault perception accuracy of deep reinforcement learning algorithm is over 95%, which has higher accuracy, smaller positioning delay and outstanding application performance compared with existing fault perception algorithms.

3. Fault Diagnosis Modeling of Communication Network Based on Deep Learning

The error characteristic data of the whole telecommunication network of intelligent power station has a large amount of data, which is not conducive to the traditional method of processing the error characteristic data one by one.

Therefore, this paper proposes a deep learning method, which creates a diagnosis model through machine learning, which represents the nonlinear mapping relationship between fault characteristics and location is shown in formula (1), and realizes fault handling and analysis. At the same time, it has high-dimensional error characteristics.

$$Y_j = f\left(X_j\right), \tag{1}$$

Where: X_j represents the j-th fault feature set; Y_j denotes the j-th communication network fault code.

3.1. Automatic Generation Method of Fault Samples. In order to realize autonomous training of deep fault diagnosis model, it is necessary to provide fault sample set for

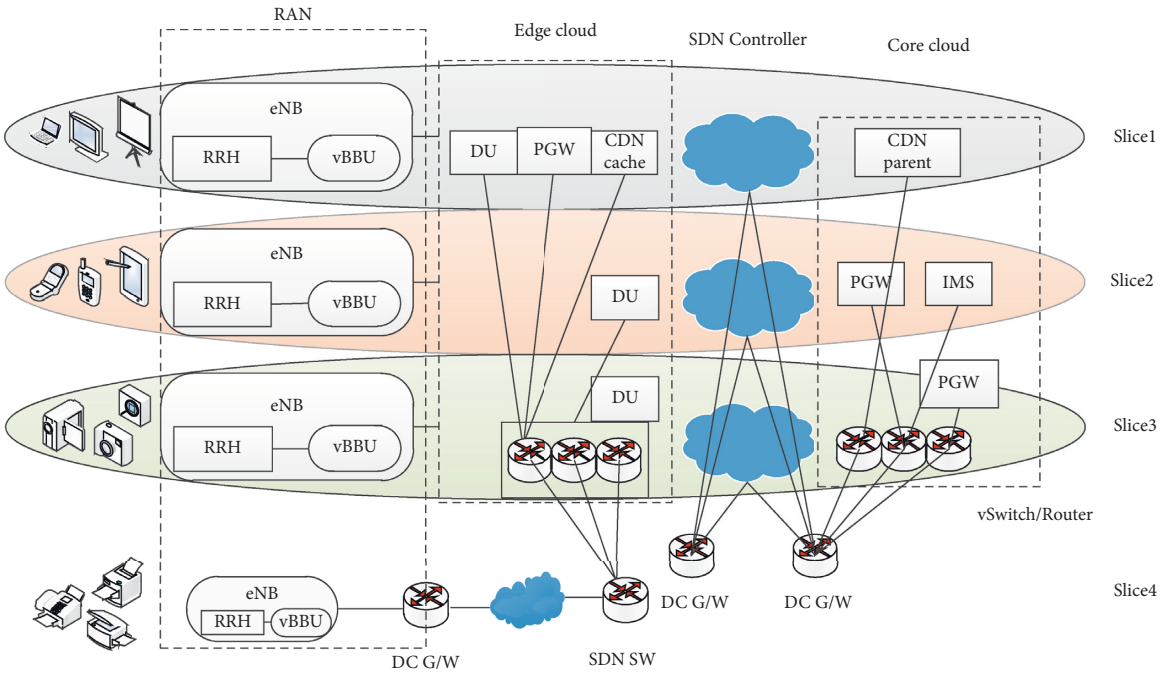

Figure 1: 5G network architecture diagram.

Table 1: 5G network failures.

Interference	Uplink interference downlink interference
Overlay vulnerability	Coverage boundary has no coverage blind spot within coverage
Hardware	Antenna failure RF transmission chain/reception chain failure other hardware failures (power supply, GPS clock module)
Transmission	Interface failure: NG interface/xn interface link failure beam fault
Network slicing	NFV fault network slicing configuration Configuration of connection resources: Over-utilization of connection resources and under-utilization of connection resources allocation of computing resources: Over-utilization of computing resources and under-utilization of computing resources memory resource configuration: Overuse of memory resources, insufficient utilization of memory resources slice interoperability network management security
Others	Fading Configuration parameter error

telecommunication network. It is very common to collect historical failures to obtain a database, but this situation requires a certain amount of accumulation time, and because of the high reliability of the equipment, the operation is insufficient in the case of equipment failure. Therefore, in addition to historical error data samples, it is necessary to automatically generate correct and reliable error samples.

According to Bessel's system definition and basic principles, this paper regards telecommunication network as a whole, and introduces external factors (such as random component failure, network topology modification, network component configuration, etc.).

$$S(t+\Delta t) = g(I(t), S(t)). \tag{2}$$

The state vector S is shown in formula

$$S = [EbrX, EvX, Pl], \tag{3}$$

Where A is the actual transmission path of the message.

The input vector I is shown in formula

$$I = \left[A, C, P, S_{\text{conponent}}, H\right]. \tag{4}$$

In the above formula, $S_{\text{conponent}}$ is the working mode of communication network components; H is the operating environment parameter of telecommunication network.

The instruction instance obtained by the generation method can be stored in the database according to a certain operation mode $x = [A, C, P]$. As shown in formula

$$\begin{cases} D = \{D_1, D_2, \ldots, D_j, \ldots, D_M\}, \\ D_j = \{X_j\}. \end{cases} \tag{5}$$

In the above formula, D_j is the j-th fault sample.

3.2. Fault Diagnosis Model Based on DBN. DBN is widely used in image recognition and other fields, because it can deal with horizontal and vertical high-dimensional input, and describe the nonlinear relationship between input and

output with multi-layer structure. In addition, due to the redundancy rate of high-dimensional data, it has good fault tolerance and can still produce accurate values when data is lost/erroneous. Therefore, this paper uses DBN to build a fault diagnosis model of communication network.

DBN is composed of several RBM stacks, and the correlation between fault characteristics and fault locations of telecommunication network is represented by several hidden layers to realize diagnosis and analysis operations. The fault features are inputted in the input layer $X_j = [x_1, x_2, \ldots, x_m]$, The output level is communication network fault location $Y_j = [y_1, y_2, \ldots, y_n]$, where N is the total number of communication network components, y_i refers to whether the i-th component in the network is faulty or not, if the component is faulty, $y_i = 1$, otherwise, it is 0.

DBN adds pre-training process through greedy unsupervised learning, that is, only using fault attribute data to preset network parameters, so as to avoid local optimal solution caused by arbitrary network parameters.

The energy function that defines RBM is shown in formula

$$E(v, h|\theta) = -\sum_{i=1}^{n_v}\sum_{j=1}^{n_h} w_{ij}v_j h_j - \sum_{i=1}^{n_v} b_i v_i - \sum_{j=1}^{n_h} c_j h_j, \quad (6)$$

Where: v_i and h_j are the neuron states of the visible layer and the hidden layer of RBM respectively, $v_i, h_j \in \{0, 1\}$; $\theta = \{c_j, b_i, w_{ij}\}$ is the RBM network parameter, where c_j and b_i are the offset values of the hidden layer and the visible layer respectively, and w_{ij} is the connection weight of the i-th visible layer neuron and the j-th hidden layer neuron; n_v and n_h are the number of neurons in visual layer and hidden layer, respectively.

According to formula (6), we can get probability distribution formula

$$P(v, h|\theta) = \frac{1}{Z(\theta)} e^{-E(v,h|\theta)}. \quad (7)$$

The CD algorithm is used to reconstruct the input layer in both positive and negative directions, as shown in formula (8) and formula (9)

$$P(h_j = 1|X) = f\left(c_j + \sum_{i=1}^{n_v} w_{ij}x_i\right), \quad (8)$$

$$P(v_i = 1|h) = f\left(b_i + \sum_{j=1}^{n_h} w_{ij}h_j\right). \quad (9)$$

The network parameters are updated according to the error, as shown by formulas (10)–(12)

$$w_{ij} = w_{ij} + \varepsilon\left[P(h_{0j} = 1|v_0)v_{i0} - P(h_{1j} = 1|v_1)v_{i1}\right], \quad (10)$$

$$b_i = b_i + \varepsilon(v_{i0} - v_{i1}), \quad (11)$$

$$c_j = c_j + \varepsilon\left[P(h_{0j} = 1|v_0) - P(h_{1j} = 1|v_1)\right], \quad (12)$$

Where ε is the learning rate.

In the fine-tuning process, the general BP algorithm is used to supervise the learning of the whole DBN. All the instruction examples are used to calculate the MSE and gradient between the DBN output layer and the target output, and adjust the network parameter θ in the opposite direction of the gradient. The objective function of optimization is shown in (13), and the matching of network parameters is shown in (14).

$$\min_{\theta} J(\theta) = \frac{1}{N}\sum_{i=1}^{N} \widehat{x}^{(i)} - x_2^{(i)2}, \quad (13)$$

$$\theta = \theta - \varepsilon \cdot \nabla_\theta J(\theta), \quad (14)$$

Where: $\widehat{x}^{(i)}$ is the diagnosis result of the i-th sample; $x^{(i)}$ is the actual fault of the i-th sample.

4. Experimental Analysis

4.1. Simulation Result Analysis. The model training is carried out on a single-core CPU computer, and the iteration times of the model training process are 5000 times. Fault detection accuracy pairs of different fault location algorithms are shown in Figure 2 and Table 2. The current algorithms are AA, GA and FA.

4.2. Analysis of Fault Location Results

4.2.1. Single Fault Location Analysis. Only one fault in the system is a single fault. By verifying the test set, we analyze the effectiveness of DNN on it. The results are shown in Tables 3 and 4.

Looking at Tables 3 and 4, we can conclude that DNN is very effective in locating various fault types.

In the process of fault location. When a failure occurs, the traffic through the switch drops rapidly, and then an abnormal traffic alarm is triggered, as shown in Table 5. In addition, because the related secondary equipment cannot receive these messages normally, It will send a message to receive an exception. Therefore, X_D and X_M composed of alarm information are represented by formulas (15) and (16).

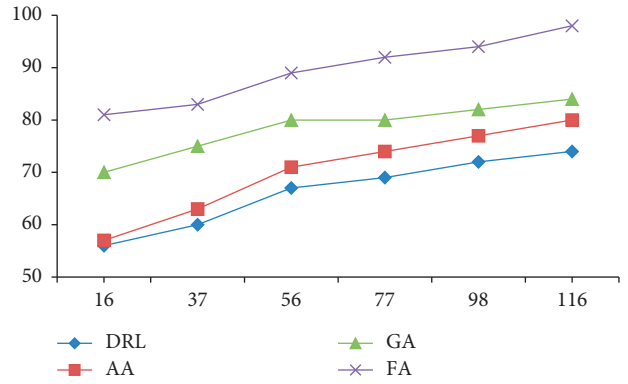

Figure 2: Accuracy of different fault awareness algorithms.

Table 2: Fault intelligent sensing performance comparison table.

Algorithm	Accuracy	Perceptual delay (ms)	Storage space	Cost	Perceived fault type	Network scale
DRL	0.95–0.99	0.30–0.40	Small	Low	Soft and hard faults	Complex network
AA	0.80–0.90	5.0–6.0	Small	Gao	Hard fault	Simple network
GA	Gao	Slow	Big	0	Soft and hard faults	Simple network
FA	Low	Quickly	Small	0	Hard fault	Simple network

$$\begin{cases} X_D = [X_{MU\_1}, X_{P\_1}, X_{P\_5}, X_{IT\_1}, X_{MC\_1}, X_{MC\_2}, X_{MC\_3}, X_{MC\_4}, X_{MC\_5}], \\ X_{MC\_1} = [A_{\text{AMR\_S13}}], \\ X_{P\_1}[A_{\text{AMR\_G56}}], X_{P\_5}[A_{\text{AMR\_G9}}, A_{\text{AMR\_S2}}], \\ X_{IT\_1} = [A_{\text{AMR\_G57}}], \\ X_{MC\_1} = [A_{\text{AMR\_G10}}, A_{\text{AMR\_G19}}, A_{\text{AMR\_G35}}, A_{\text{AMR\_G51}}], X_{MC\_2} = [A_{\text{AMR\_G3}}], \\ X_{MC\_3} = [A_{\text{AMR\_G4}}], X_{MC\_4} = [A_{\text{AMR\_G5}}], X_{MC\_5} = [A_{\text{AMR\_G6}}], \end{cases} \tag{15}$$

$$\begin{cases} X_M = [S_1, S_2, S_3, S_4, S_5], \\ S_1 = [P_4], P_4 = \begin{bmatrix} A_{\text{AMT\_G10}}, A_{\text{AMT\_G19}}, A_{\text{AMT\_G35}}, A_{\text{AMT\_G51}}, \\ A_{\text{AMT\_G56}}, A_{\text{AMT\_G57}}, A_{\text{AMT\_S13}} \end{bmatrix}, \\ S_2 = [P_{17}], P_{17} = [A_{\text{AMT\_G3}}], \\ S_3 = [P_{29}], P_{29} = [A_{\text{AMT\_G4}}], \\ S_4 = [P_{53}], P_{53} = [A_{\text{AMT\_G5}}], \\ S_5 = [P_{79}], P_{79} = \begin{bmatrix} A_{\text{AMT\_G3}}, A_{\text{AMT\_G4}}, A_{\text{AMT\_G5}}, A_{\text{AMT\_G6}}, \\ A_{\text{AMT\_G9}}, A_{\text{AMT\_S2}} \end{bmatrix}. \end{cases} \tag{16}$$

The formed X is used as the input of the DNN model, the obtained failure result is shown in the formula.

$$Y_{\text{DNN}} = \begin{bmatrix} L2 \\ 0, \ldots, 1, \ldots, 0 \end{bmatrix}. \tag{17}$$

Cross-link method locates communication network faults only according to message receiving status. In this example, the fault location result obtained due to the failure of the associated secondary device to normally receive the message is shown in.

$$Y = \begin{bmatrix} L2\ \text{Port}_4\ \text{Port}_{79} \\ 0, \ldots, 1, \ldots, 1, \ldots, 1, \ldots, 1, \ldots, 0 \end{bmatrix}. \tag{18}$$

The traffic determination method locates a communication network fault based only on a state, resulting in a fault location result as shown in.

Table 3: Fiber link failure.

Link number	Accuracy (%)
L1	98.795
L2	97.597
L3	98.889
L4	98.824
L5	98.851
L6	100
L7	100
L8	98.667
L9	97.647
L10	98.864
L11	99.765
L12	98.75
L13	100
L14	100
L15	98.611
L16	97.727
L17	98.718
L18	98.757
L19	99.78
L20	99.023
L21	100
L22	98.63
L23	100
L24	99.795
L25	100
L26	100
L27	100
L28	99.864
L29	97.778
L30	99.75
L31	98.756
L32	99.81
L33	99.718
L34	98.592
L35	98.684
L36	100
L37	100
L38	100
L39	100
L40	100
L41	97.856
L42	98.847
L43	98.649
L44	99.897
L45	100
L46	100

$$Y = \begin{bmatrix} L2\mathrm{Port}_2\mathrm{Port}_4\mathrm{Port}_{79} \\ 0, \cdots, 1, \cdots, 1, \cdots, 1, \cdots, 1, \cdots, 0 \end{bmatrix}. \quad (19)$$

To compare the effects of fault location, we use the same evaluation index.

Observing the calculation results, the result of the method proposed in this chapter is 0. The method proposed in this chapter can reduce the scope of suspicious faults and improve the efficiency of operation and maintenance.

According to the above calculation method, the obtained data are as shown in the following Table 6.

Observing the above table, we can conclude that the results of the model proposed in this paper are lower than the other two models, so it can effectively improve the accuracy of fault location. DNN can achieve this effect because it is more reasonable in data processing.

4.2.2. Multiple Fault Location Analysis. There are multiple faults in the system at the same time, which is called multiple faults. These faults can be located in one position or in different positions.

Table 4: Equipment port failure.

Port number	Accuracy (%)
1	98.81
2	99.547
3	97.684
4	98.734
5	97.611
6	98.667
7	98.876
8	100
9	97.824
10	100
11	100
12	100
13	99.876
14	99.845
15	97.653
16	97.63
17	98.663
18	97.834
19	99.546
20	98.901
21	100
22	98.734
23	100
24	100
25	100
26	97.789
27	99.436
28	97.453
29	97.845
30	99.765
31	97.463
32	99.676
33	98.701
34	97.563
35	97.667
36	97.925
37	100
38	100
39	98.645
40	98.463
41	100
42	98.245
43	100
44	97.753
45	100
46	100
47	100
48	100
49	100
50	100
51	98.887
52	97.782
53	99.453
54	98.837
55	99.78
56	99.667
57	98.567
58	98.531
59	98.788
60	97.564

Table 4: Continued.

Port number	Accuracy (%)
61	98.75
62	100
63	97.328
64	100
65	100
66	98.628
67	97.564
68	100
69	99.653
70	100
71	100
72	100
73	100
74	100
75	100
76	97.738
77	98.901
78	97.678
79	99.474
80	97.757
81	98.649
82	99.634
83	97.257
84	99.731
85	97.784
86	99.837
87	100
88	98.554
89	100
90	100
91	99.63
92	100

Table 5: Messages failed by L2.

Switch	Port	Message
1	4	G10, G19, G35, G51, G56, G57, S13
2	17	G3
3	29	G4
4	53	G5
5	79	G3, G4, G5, G6, G9, S2

Table 6: Error comparison.

Fault location method	Accuracy of fault location (%)	Maximum error	Minimum error	Average error
DNN	99.072	0.5	0	0.004
Cross link method	80.692	0.889	0	0.249
Flow judgment method	77.644	0.875	0	0.314

Table 7: Messages affected by failures.

Switch number	Port number	Message number
1	3	S1, S2
	4	G56, G57
2	17	G58, G59
3	29	G60, G61, G62
4	53	G63, G64, G65
5	79	G3, G4, G5, G6, G9, S2
	85	G56, G57, G58, G59, G60, G61, G62, G63, G64, G65

When a failure occurs, the traffic of the switch will drop rapidly, thus triggering a traffic alarm, and the results are shown in Table 7; because the relevant secondary equipment cannot receive these messages normally, It will also give an abnormal alarm; In addition, the merging unit 1 and the protection device 5 will issue a device abnormality alarm. Thus, X_D and X_M in the fault feature set X constituted by the alarm information are shown by formulas (20) and (21).

$$\begin{aligned} X_D &= \begin{bmatrix} X_{MU\_1}, X_{P\_1}, X_{P\_2}, X_{P\_3}, X_{P\_4}, X_{P\_5}, X_{IT\_1}, \\ X_{IT\_2}, X_{IT\_3}, X_{IT\_4}, X_{IT\_6}, X_{IT\_7} \end{bmatrix}, \\ X_{MU\_1} &= [A_{\mathrm{STE}}, A_{\mathrm{AMR\_}G1}, A_{\mathrm{AMR\_}G8}, A_{\mathrm{AMR\_}S1}, A_{\mathrm{AMR\_}S13}], \\ X_{P\_1}&[A_{\mathrm{AMR\_}G56}], X_{P\_2}[A_{\mathrm{AMR\_}G58}], X_{P\_3}[A_{\mathrm{AMR\_}G61}], X_{P\_4}[A_{\mathrm{AMR\_}G64}], \\ X_{P\_5}&\begin{bmatrix} A_{\mathrm{STE}}, A_{\mathrm{AMR\_}G9}, A_{\mathrm{AMR\_}G18}, A_{\mathrm{AMR\_}G31}, A_{\mathrm{AMR\_}G34}, A_{\mathrm{AMR\_}G47}, A_{\mathrm{AMR\_}G50} \\ , A_{\mathrm{AMR\_}S2}, A_{\mathrm{AMR\_}S4}, A_{\mathrm{AMR\_}S6}, A_{\mathrm{AMR\_}S8}, A_{\mathrm{AMR\_}S10}, A_{\mathrm{AMR\_}S12} \end{bmatrix}, \\ X_{IT\_1} &= [A_{\mathrm{AMR\_}G57}], X_{IT\_2} = [A_{\mathrm{AMR\_}G59}], X_{IT\_3} = [A_{\mathrm{AMR\_}G60}], \\ X_{IT\_4} &= [A_{\mathrm{AMR\_}G62}], X_{IT\_6} = [A_{\mathrm{AMR\_}G63}], X_{IT\_7} = [A_{\mathrm{AMR\_}G65}], \end{aligned} \tag{20}$$

$$\begin{cases} X_M = [S_1, S_2, S_3, S_4, S_5], \\ S_1 = [P_3, P_4], P_3 = [A_{\mathrm{AMT\_}S1}, A_{\mathrm{AMT\_}S2}], P_4 = [A_{\mathrm{AMT\_}S56}, A_{\mathrm{AMT\_}S57}], \\ S_2 = [P_{17}], P_{17} = [A_{\mathrm{AMT\_}G58}, A_{\mathrm{AMT\_}G59}], \\ S_3 = [P_{29}], P_{29} = [A_{\mathrm{AMT\_}G60}, A_{\mathrm{AMT\_}G61}, A_{\mathrm{AMT\_}G62}], \\ S_4 = [P_{53}], P_{53} = [A_{\mathrm{AMT\_}G63}, A_{\mathrm{AMT\_}G64}, A_{\mathrm{AMT\_}G65}], \\ S_5 = [P_{79}, P_{85}], P_{79} = [A_{\mathrm{AMT\_}S2}], \\ P_{85} = \begin{bmatrix} A_{\mathrm{AMT\_}G56}, A_{\mathrm{AMT\_}G57}, A_{\mathrm{AMT\_}G58}, A_{\mathrm{AMT\_}G59}, A_{\mathrm{AMT\_}G60}, A_{\mathrm{AMT\_}G61}, \\ A_{\mathrm{AMT\_}G62}, A_{\mathrm{AMT\_}G63}, A_{\mathrm{AMT\_}G64}, A_{\mathrm{AMT\_}G65} \end{bmatrix}. \end{cases} \tag{21}$$

Enter the fault feature set in DNN, and the result is shown in formula.

$$Y_{\mathrm{DNN}} = \begin{bmatrix} P_7 P_{88} \\ 0, \ldots, 1, \ldots, 1 \ldots, 0 \end{bmatrix}. \tag{22}$$

According to the above analysis process, the state of two ports is used for fault location. However, because the links sent by the two ports do not intersect, the result of positioning is an empty set.

The result is expressed by

$$Y = \begin{bmatrix} L3L43P3P7P85P88 \\ 0, \ldots, 1, \ldots, 1 \ldots, 1, \ldots, 1, \ldots, 1, \ldots, 1, \ldots, 0 \end{bmatrix}. \tag{23}$$

100 sets of data samples were obtained by randomly simulating various complex fault scenarios to the effectiveness of this method in multi-fault environment is verified. Using the model mentioned above, the errors of all samples are calculated, and the results are shown in the following Tables 8 and 9.

4.3. Network Fault Detection and Diagnosis Results. Using the network fault detection and diagnosis idea based on AWGAN-GP proposed in this section, after selecting the function, the AWGAN-GP algorithm is used to learn the sample data collected from the real network environment according to certain rules. In any network mode. Obtain a large amount of analog data with labels anywhere in the network. In the fault diagnosis model, the real data is used as the test data to test the model. In addition, the virtual data generated by the generated resistance network is used as training data to train the fault detection and diagnosis model. In order to better prove that the algorithm can produce reliable virtual data, several classical classification

Table 8: Error comparison of two kinds of fault location when multiple faults occur.

Fault location method	Accuracy of fault location (%)	Maximum error	Minimum error	Average error
DNN	92	0.333	0	0.027
Cross link method	41	1	0	0.558
Flow judgment method	0	1	0.333	0.607

Table 9: Error comparison of triple fault location methods when multiple faults occur.

Fault location method	Accuracy of fault location (%)	Maximum error	Minimum error	Average error
DNN	86	0.25	0	0.035
Cross link method	36	1	0	0.632
Flow judgment method	0	1	0.25	0.694

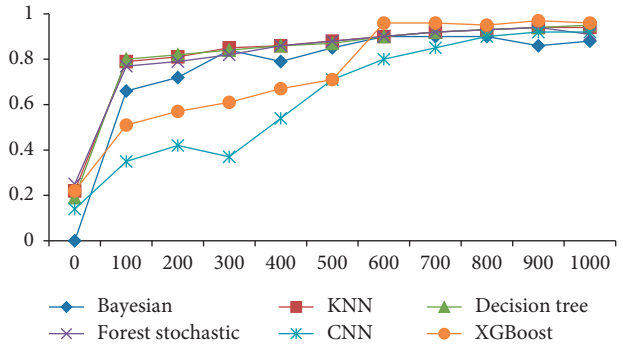

Figure 3: Accuracy of each fault diagnosis model after feature screening.

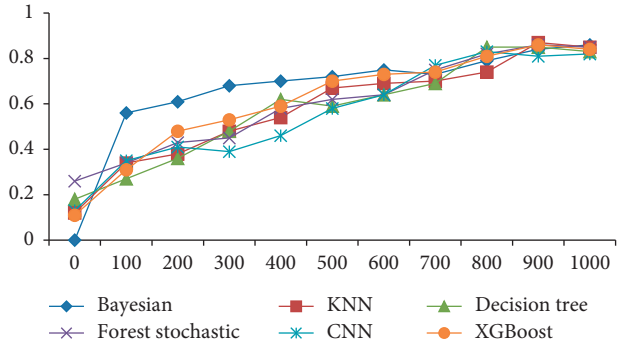

Figure 4: Accuracy of each fault diagnosis model without feature screening.

algorithm models are selected in the fault diagnosis model of this chapter for verification.

First of all, this section takes the simulation data and original data generated before and after work screening as training data and simulation data respectively, and practices and tests various fault diagnosis models. The simulation results are shown in Figures 3 and 4. Continuous iteration makes the performance of each classification algorithm more stable, and the fault diagnosis accuracy of each classification model before and after applying feature screening is sorted according to Table 10. As can be seen from the table, each fault diagnosis model is carried out after function screening. The accuracy of error diagnosis is higher than that of the untrained feature screening model, which shows that although the original small sample size is increased by the creation of the final simulation sample, the distribution of

Table 10: Comparison of accuracy of fault diagnosis models before and after feature screening after training stabilization.

Accuracy	Algorithm					
	Bayesian (%)	KNN (%)	Decision tree (%)	Forest stochastic (%)	CNN (%)	XGBoost (%)
After feature screening	92.37	97.11	98.87	98.48	97.33	98.92
Before feature screening	89.01	87.44	88.10	88.22	84.31	91.26

Table 11: Comparison of fault diagnosis time.

Time	Algorithm					
	Bayesian	KNN	Decision tree	Forest stochastic	CNN	XGBoost
After feature screening	0.44	0.28	0.37	0.36	1.24	0.28
Before feature screening	0.67	0.31	0.46	0.44	2.1	0.34

the generated data is not consistent with the original data set. Therefore, if we can filter out the virtual samples that violate the distribution law of the original data set, we can effectively improve the classification accuracy of the next classifier.

On the other hand, considering the time of detecting and diagnosing network faults, after function screening, the input parameters of the training model are reduced, and the learning time of the model is also reduced accordingly. The final time for troubleshooting is shown in Table 11. The process described in this chapter takes less time to diagnose network errors after feature filtering than it does without filtering functionality during troubleshooting. In view of the accuracy and timing of the network fault detection and diagnosis model, this chapter finally chooses XGBoost model as the final network fault detection and diagnosis model.

The results show that the model proposed in this paper can locate the fault location more accurately when dealing with higher dimensional feature sets; In addition, under the influence of feature information loss or false positives, DNN can still accurately locate fault points because of its excellent stability.

5. Concluding

The secondary system composed of secondary equipment and telecommunication network is the basic requirement for the normal operation of intelligent substation. At present, there are many shortcomings in the method of positioning secondary substation in intelligent substation. It is mainly manifested in the weak ability of state data processing, low accuracy of fault location and poor anti-interference ability. In this paper, based on the existing research, a new intelligent fault location method is proposed. In order to overcome the difficulties encountered in the process of intelligent substation troubleshooting, we adopt a new method. This paper presents a method based on DNN. Firstly, fault status redundancy monitoring analyzes the characteristic data received by each control node in different positions, and proposes the presentation of fault characteristic information. Secondly, because of the application of this principle, a large number of samples will be generated, which will enlarge the training samples. Finally, combined with deep learning, the model is established.

Data Availability

The experimental data used to support the findings of this study are available from the corresponding author upon request.

Conflicts of Interest

The authors declare that they have no conflicts of interest.

Acknowledgments

This work was sponsored in part by Industry University Cooperation Collaborative Education Project (202102453006).

References

[1] S. Yi, X. Wang, and X. Tang, "Deep learning face representation from predicting 10,000 classes," in *Proceedings of the IEEE Conference on Computer Vision & Pattern Recognition*, June 2014.

[2] C. Zhang, S. Bengio, M. Hardt, B. Recht, and O. Vinyals, "Understanding deep learning requires rethinking generalization," vol. 2, no. 5, pp. 321–372, 2016, https://arxiv.org/abs/1611.03530.

[3] G. Litjens, T. Kooi, B. E. Bejnordi et al., "A survey on deep learning in medical image analysis," *Medical Image Analysis*, vol. 42, no. 9, pp. 60–88, 2017.

[4] B. Alipanahi, A. Delong, and M. T. Weirauch, "Predicting the sequence specificities of DNA- and RNA-binding proteins by deep learning," *Nature Biotechnology*, vol. 37, no. 22, pp. 5827–5893, 2015.

[5] F. Chollet, "Xception: deep learning with depthwise separable convolutions," *IEEE*, vol. 1, no. 4, pp. 69–91, 2017.

[6] C. R. Qi, H. Su, and K. Mo, "PointNet: deep learning on point sets for 3D classification and segmentation," *IEEE*, vol. 16, no. 11, pp. 215–278, 2017.

[7] J. Weston, F. Ratle, and H. Mobahi, "Deep learning via semi-supervised embedding," *ACM*, vol. 7, no. 42, pp. 4829–4901, 2008.

[8] Y. Lv, Y. Duan, W. Kang, and Y. Duan, "Traffic flow prediction with big data: a deep learning approach," *IEEE Transactions on Intelligent Transportation Systems*, vol. 16, no. 2, pp. 865–873, 2015.

[9] X. Fei and G. Z. Tian, "Optimization of communication network fault identification based on NB-IoT," *Microprocessors and Microsystems*, vol. 80, Article ID 103531, 2021.

[10] X. Liang and C. Huang, "Wavelet-based SNR analysis in building satellite terminal fault identification system," in *Proceedings of the 2008 IEEE International Conference on Communications*, May 2008.

[11] M. Zheng, J. Yu, and X. Ding, *Application of Big Data Technology In Protection Channel Interruption Analysis And Breaker Defect Identification*, Springer, Berlin, Germany, 2020.

[12] J. Choi, M. Choi, and S. H. Lee, "An alarm correlation and fault identification scheme based on osi managed object classes," in *Proceedings of the IEEE International Conference on Communications*, June 1999.

[13] Z. H. Dai, Z. P. Wang, and Y. J. Jiao, "Reliability evaluation of the communication network in wide-area protection," *IEEE Transactions on Power Delivery*, vol. 26, no. 4, pp. 2523–2530, 2011.

[14] C. C. Lo and S. H. Chen, "Robust event correlation scheme for fault identification in communication networks," *International Journal of Communication Systems*, vol. 12, no. 3, pp. 217–228, 1999.

[15] H. Peng, "Simulation of fault data recognition method in underwater ship communication network," *Microelectronics & Computer*, vol. 18, no. 5, pp. 282–328, 2016.